

Article

Microstructural Analysis and Tribology Behavior of a Medium-Mn Steel with Mo

Benito Del Río López ¹, Ana García Díez ^{2,*} , José Luís Mier Buenhombre ², Carolina Camba Fabal ² and Almudena Filgueira Vizoso ²

¹ Escuela Técnica Superior de Ingenieros Industriales, Polytechnic University of Madrid, José Gutiérrez Abascal n°2, 28006 Madrid, Spain; bdelrio@etsii.upm.es

² Escuela Politécnica Superior, University of A Coruña, Mendizábal s/n, 15403 Ferrol, Spain; jlmier@udc.es (J.L.M.B.); ccamba@udc.es (C.C.F.); almudena@udc.es (A.F.V.)

* Correspondence: ana.gdiez@udc.es; Tel.: +34-881-013-221

Received: 10 September 2018; Accepted: 19 September 2018; Published: 21 September 2018



Abstract: This paper presents an alternative to the materials traditionally used in the manufacture of coal mills for coating wedges. For this purpose, we designed and tested ten new austenitic steels with medium manganese content. The thermal structural stability and hardness were evaluated after different heat treatments. The steels were subjected to hyperquenching and tempering between 100 and 900 °C. A metallographic analysis of each sample was then performed to determine their thermal stability, and the Brinell hardness was measured. Later, wedges of two alternatives and reference-material alloys were manufactured and installed in three types of mills. Their mass loss was determined after 25 months and at an intermediate time during that period. One steel was selected as an alternative material.

Keywords: manganese steel; abrasive wear; thermal treatments; hardness

1. Introduction

The importance of wear-resistant alloys under different service conditions (adhesion, abrasion, erosion, impact, temperature, etc.) is well-known in industry. Many alloys have been developed to provide a technical and economic response to various industrial problems, and ferrous alloys are undoubtedly the most suitable in many cases for their low price, good performance, the great number of commercial alloys they provide, their accessibility, and diversity of possible microstructures.

Manganese austenitic steels, also known as Hadfield steels, are among the ferrous alloys most used under severe wear conditions in the presence of impacts at low temperatures. There are numerous works evaluating the properties of these types of steel [1–4], the transformation phenomenon of retained austenite in martensite [5–7], and the influence of the service deformation processes on the properties and microstructure [8–10]. However, these steels suffer accelerated wear when the working temperature is above 100 °C due to carbide precipitation and subsequent loss of hardness. In these cases, Hadfield steels are traditionally replaced by pearlitic steels or low/medium alloy tempered steels [11].

Austenitic steels with molybdenum and a low manganese content have obvious advantages over pearlitic and martensitic steels. They are very attractive for certain applications in which Hadfield steels with 14% Mn, pearlitic steels and martensitic steels all offer an unsatisfactory performance, especially at service temperatures between 100 and 400 °C and under the influence of impact and abrasion [12–14]. Under these conditions, pearlitic steels suffer accelerated wear, and martensitic steels may undergo cracking.

The wedges utilized in ball mills which are used in conventional coal-fired power plants are an example of these types of alloy. The function of these wedges is critical in the milling of coal,

and therefore the particle size obtained and the burners' performance [15]. These wedges are subjected to impact and abrasion conditions, and must have a certain toughness to prevent cracking during service and fracture in assembly. The amount of torque they must withstand means that materials with hardness greater than 400 HB are inadequate, and materials with a hardness of less than 300 HB suffer unacceptable wear. The working temperature of the mill is another factor to consider when proposing a new material for this purpose. Depending on the installation, this temperature usually varies between 80 and 150 °C [16–18]. Another factor to consider in the choice of material used in the mill wedges is their service life. Since the required service life for usage in these mills is usually near two years, the softening of tempered construction steels as well as quenched and tempered tool steels is noticeable, due to the impact of both time and temperature [19].

This paper studies the response of austenitic medium-manganese steels to impact and high-temperature wear, as well as their service performance in coal mills.

2. Materials and Methods

2.1. Casting

Ten castings with different carbon, manganese, chromium, molybdenum, and copper contents were designed. Their chemical composition was based on prior knowledge of the alloy elements of austenitic manganese steels, and on the results achieved in previous castings [20–23].

The melting and casting into molds was performed using a middle-frequency induction furnace (3000 Hz) with a capacity of 50 kg of crucible steel. A neutral refractory coating was used for both the furnace and the ladle. Because of the high basicity of slag and this molten steel, it is necessary to reduce or eliminate degradation due to the reaction of these substances with the furnace refractory and the molding sand. All samples were subjected to hyperquenching in air from 1100 °C. The residence time at this temperature was two hours. Heating at such a high temperature counteracts the risk of possible austenite decomposition introduced by the use of this very long residence time. Two hours is long enough to achieve the correct solubilization. A longer residence time is necessary for complete dissolution, but this has no industrial application. This paper proves that as long as the thickness did not exceed 150 mm, air cooling was sufficient to prevent the appearance of precipitates. Typical Hadfield steel of such a thickness requires water quenching to harden completely. That is, the steels studied in this work have more hardenability. Thereafter, tempering was carried out between 100 and 900 °C at intervals of 50 °C for two hours to study the stability of austenite in these types of steel.

Figure 1 shows the cycle used in the different heat treatments.

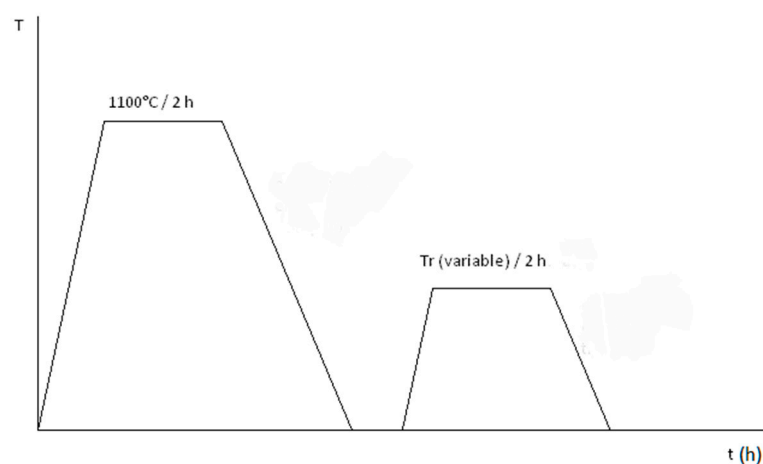


Figure 1. Diagram of the thermal treatment carried out.

2.2. Sample Preparation and Metallographic Analysis

Metallographic specimens for analysis were obtained from molded internal supply ducts. The diameter of these ducts was 15 mm, thus allowing for sample mounting after adequate cooling and cutting with a metallographic cut-off machine. After manual grinding and polishing, samples were etched at room temperature with a 3% nital etchant. The etching was performed for only a short duration, as this prevents the rapid overstretching of high manganese austenite, which leads to excessive coloring of the matrix as well as detrimental effects for the microscopic examination of the dispersed microconstituent.

The metallographic study was completed with a hardness measurement. In each sample, five measures of the Brinell hardness using a 10 mm diameter ball and a load of 3000 kg were taken. Hardness in these steels is quite important because it allows qualitative estimation of the austenite decomposition in other constituents. The austenite of these steels is by far the softest constituent, and therefore any significant increase in hardness above 220–250 HB in the absence of cold working can be interpreted as due to the decomposition of austenite [1].

2.3. In-Service Tests

Due to the limitations in testing these wedges in the mills, a pre-selection was made according to the hardness and metallography results obtained in the laboratory, reducing the number of alloys tested in service to two. These were then tested together with the material usually used. It was necessary to ensure there was an austenitic structure at the service temperature of the mill. The austenitic structure was also necessary to ensure hardening during the service of these alloys, as well as being able to present fragile fractures on account of the impact of the mill balls [24].

Wedges made of two of the alloys studied in this article were installed in the coal ball mill of a power generating company in order to quantitatively evaluate their wear resistance. These two alloys were determined as the most convenient according to the previous studies.

Wedges made of both the proposed and commercial alloys were manufactured for this application, and the same shape as the original mill was retained. There were ten wedges of each type of material. The operating period was 25 months, and an intermediate weight loss control was carried out during the short mill downtimes motivated by incidents in service. After this time, all of the wedges were dismantled to conduct a study of weight loss and wear profiles. A visual inspection of the wear profiles was performed to confirm that there was no macroscopic plastic deformation to prevent the operation of the wedges without mass loss.

3. Results and Discussion

3.1. Chemical Analysis

The chemical composition of the ten proposed castings is detailed in Table 1. All compositions had values of phosphorus and sulfur that were less than 0.025%.

Table 1. Chemical composition of the proposed castings (wt.%).

Casting	1	2	3	4	5	6	7	8	9	10
C	1.5	1.3	1.3	1.0	1.5	1.5	1.7	1.7	1.8	1.6
Mn	8.0	6.0	6.0	5.0	4.0	6.0	7.0	6.0	8.0	6.5
Si	0.5	0.5	0.6	0.5	0.5	0.2	0.5	0.3	0.5	0.5
Cu	2.0	2.0	3.0	3.0	3.0	3.0	2.0	2.0	2.0	2.0
Mo	2.0	1.5	1.1	1.5	2.0	2.0	2.0	1.5	2.0	1.7
Cr	1.0	2.0	0.0	0.0	0.0	0.0	1.0	1.0	1.5	1.5

3.2. Hardness

The hardness of the different alloys was measured using the Brinell scale after the corresponding hardening and tempering treatments were carried out. The data shown below correspond to the average value obtained for each alloy and heat treatment.

Figure 2 shows hardness versus tempering temperature. The zero value for the x-axis corresponds to the sample which was hyperquenched in air and did not undergo subsequent tempering.

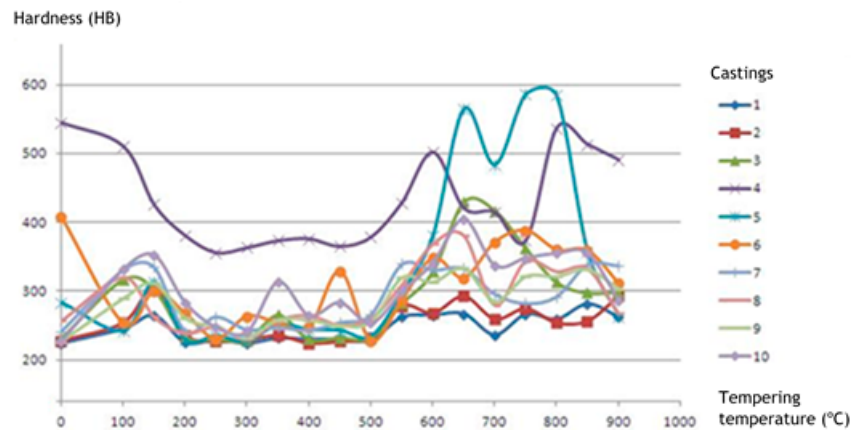


Figure 2. Hardness versus tempering temperature. The zero value for the x-axis corresponds to the sample which was hyperquenched in air and did not undergo subsequent tempering.

As shown in Figure 3, castings with a high transformation of austenite in other constituents were removed to better observe the general behavior of manganese steels [25], otherwise their properties would be similar to those of non-deformable tool steels. Every alloy experienced slight hardening in the treatment at 100–150 °C, while others were more pronounced from 550 °C, except for castings 1 and 2 which maintained a hardness of lower than 300 HB at these temperatures. It was observed that castings 7 and 9 had a similar hardness to castings 1 and 2, but with slightly higher values. Alloys 1 and 2 had the lowest hardness values in all treatments. This hardening was due to the formation of new constituents, which is studied in the metallographic analysis of the samples. The first hardening can be explained by the same mechanisms as those occurring in the tempering of high-strength steels: the appearance of fine carbide precipitates which coalesce when the temperature is increased [26].

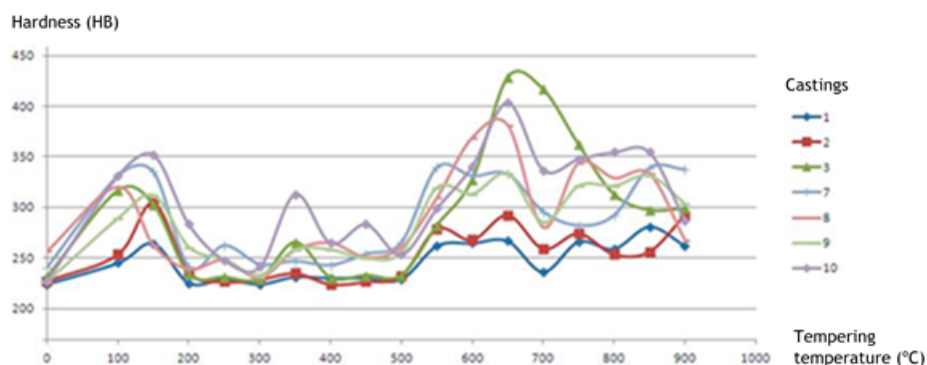


Figure 3. Detail of Figure 2 without castings 4–6, which showed a high transformation of austenite in other constituents.

3.3. Metallographic Analysis

Figure 4 shows some of the more than 500 micrographs taken in this work. Metallographic analysis revealed that the increase in hardness was related to the transformation of austenite in other constituents.

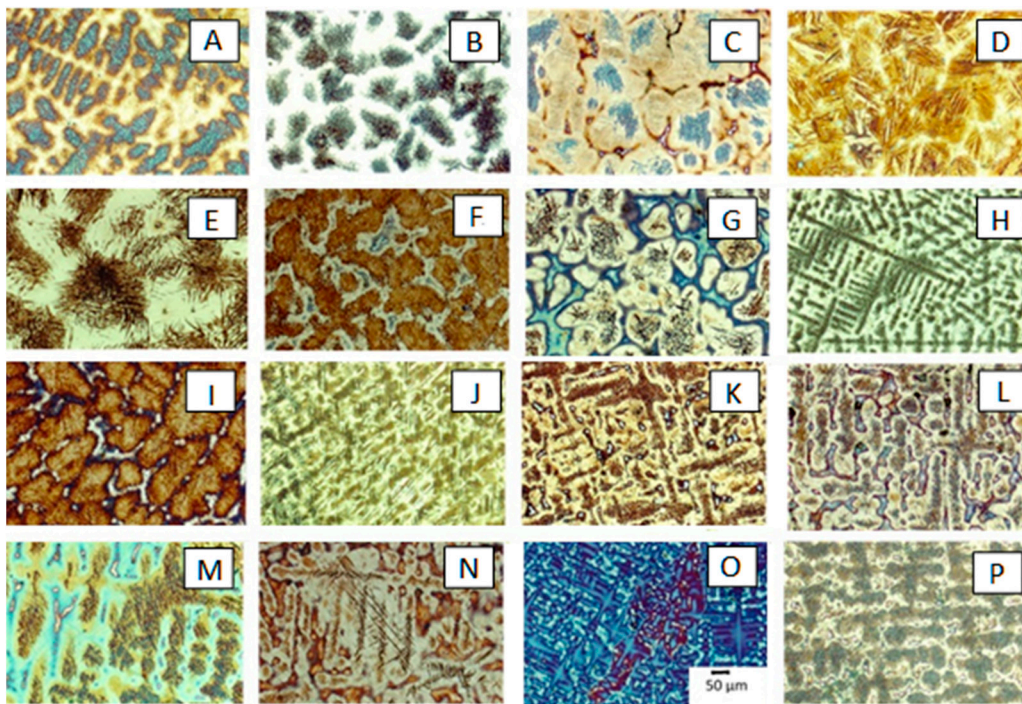


Figure 4. Examples of micrographs obtained after heat treatment: (A) casting 1, tempered at 150 °C; (B) casting 2, tempered at 550 °C; (C) casting 2, tempered at 850 °C; (D) casting 3, tempered at 100 °C; (E) casting 3, tempered at 200 °C; (F) casting 3, tempered at 800 °C; (G) casting 3, tempered at 850 °C; (H) casting 5, tempered at 250 °C; (I) casting 5, tempered at 800 °C; (J) casting 6, tempered at 100 °C; (K) casting 7, tempered at 850 °C; (L) casting 7, tempered at 900 °C; (M) casting 8, tempered at 250 °C; (N) casting 8, tempered at 750 °C; (O) casting 9, tempered at 800 °C; (P) casting 10, tempered at 900 °C.

Figure 5 shows the micrographs of the two pre-selected alloys for in-service tests.

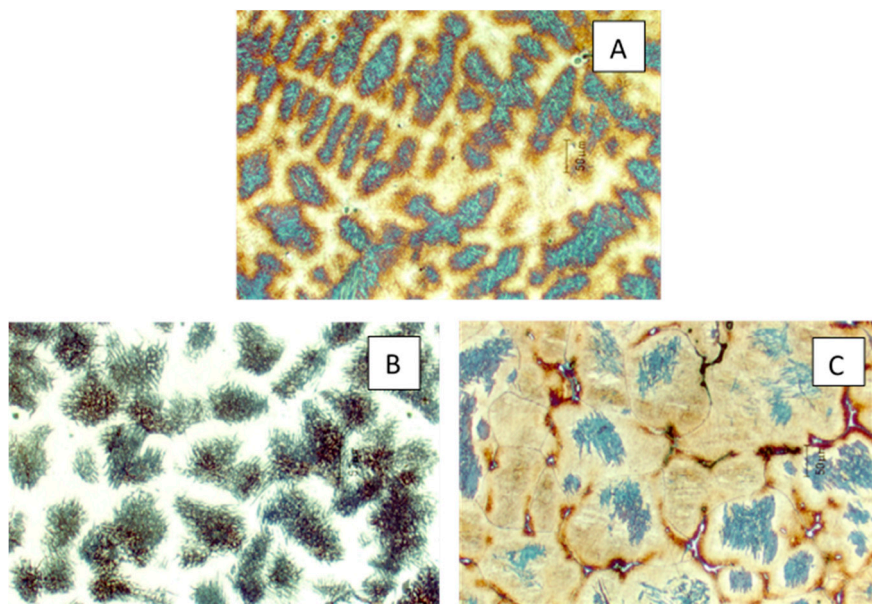


Figure 5. Examples of micrographs obtained after heat treatment: (A) casting 1, tempered at 150 °C; (B) casting 2, tempered at 550 °C; (C) casting 2, tempered at 850 °C.

The first classification of the steels depends on their hyperquenching structure. Castings 4 and 6 had high amounts of martensite, while Figure 5 shows they also contained a great amount of pearlite and bainite, which excludes these alloys from this work.

The other castings showed a large amount of retained austenite, with some cases of isolated carbides that precipitated in interdendritic positions, and small quantities of other constituents within the dendrites, which were acceptable in all cases. The increase in hardness between 100 and 150 °C may be due to the occurrence of a similar effect in the tempering of the steel at the same temperatures, but the particles were not visible by light microscopy.

The metastable austenite of the less-stable steel was transformed into lower bainite at low temperatures, and upper bainite at intermediate temperatures. The amount of bainite was scarce and isolated, so its influence on hardness was low, except in casting 10.

The most important transformation occurred between 550 and 900 °C where carbides and lamellar constituents appeared [27–29]. As a result of this, there was an increase of hardness as shown in Figures 2 and 3. A hardening appeared in some castings without the formation of new constituents, which may be possible thanks to similar secondary hardening mechanisms of high alloy tool steels.

Martensite also appeared in some castings. Carbide precipitation and reverse diffusion can decrease the content of carbon and alloying elements in austenite, leading to this phenomenon. This effect is similar to that which occurs in tool steels with very stable austenite during the first tempering. This kind of austenite is responsible for an increase in hardness and brittleness during cooling due to its transformation into martensite. This effect was more pronounced around 600–750 °C. Diffusion was much slower at lower temperatures, and at high temperatures the trend was the redissolution of possible precipitates and the homogenization of austenite. The greatest effect occurred in casting 5, which had a lower manganese content. Above 750 °C, austenitic islets reappeared in the former interdendritic spaces, which were more abundant as the temperature increased—this corresponds to the entry in the austenite, ferrite and carbides zone of the phase diagram.

3.4. Selection of In-Service Test Specimens

Manganese austenitic steel should have a predominantly austenitic structure in the operating conditions of the mill in order to achieve a good service performance. The austenitic structure is necessary to ensure toughness and avoid brittle fracture. This material has to maintain a low hardness at temperatures above the standard operating temperature for a short time. The massive precipitation of a brittle microconstituent should also be avoided to maintain the toughness of the mill wedges. Among those analyzed in this paper, alloys 1 and 2 best fit the above requirements.

3.5. In-Service Tests

Alloy 1, alloy 2, and commercial material (alloy 0) wedges were tested in three mills. Ten different wedges were tested for each alloy, and the weight loss at two different service times was measured.

Figure 6 shows an example of the wedges tested for the two selected alloys.



Figure 6. Wedges corresponding to alloys 1 and 2.

Table 2 shows the wear rate of the twenty tests performed for each of the three different materials.

Table 2. Wear rates in service.

Casting	Wear Rate (mg/h)									
Alloy 0	198.38	219.13	182.19	211.03	241.77	194.02	203.07	170.14	244.81	299.72
	202.87	217.23	209.16	251.63	189.17	208.94	179.35	161.5	168.29	187.47
Alloy 1	192.81	157.89	172.06	207.49	197.04	208.01	176.73	184.14	216.38	221.77
	248.43	226.84	228.5	262.07	244.28	276.03	221.52	278.3	201.65	209.66
Alloy 2	126.01	112.35	189.27	137.65	133.64	166.3	157.24	162.73	172.58	180.59
	172.62	175.82	252.11	227.55	187.73	220.8	254.1	192.16	172.8	172.55

A two-sample t -test (hypothesis test for the difference between two means) was conducted to see if there was any significant statistical difference between the wear rates of the three alloys. The means were equal in the null hypothesis, but different in the alternative one. As the variances were different, the total variance was estimated as the sum of the other two, while the approximate degrees of freedom were calculated with the Welch-Satterthwaite equation [30]:

$$v = \frac{\left(\frac{S_1^2}{N_1} + \frac{S_2^2}{N_2}\right)}{\frac{S_1^4}{N_1^2 \cdot v_1} + \frac{S_2^4}{N_2^2 \cdot v_2}} = \frac{\left(\frac{S_1^2}{N_1} + \frac{S_2^2}{N_2}\right)^2}{\frac{S_1^4}{N_1^2 \cdot (N_1 - 1)} + \frac{S_2^4}{N_2^2 \cdot (N_2 - 1)}}. \quad (1)$$

A t value was obtained from these degrees of freedom and a level of significance of $\alpha = 0.05$ A confidence interval for the mean difference was then obtained, which was distributed according to a Student's t -test (Welch's t -test):

$$t = \frac{\bar{X}_1 - \bar{X}_2}{\sqrt{\frac{S_1^2}{N_1} + \frac{S_2^2}{N_2}}}. \quad (2)$$

Thus, the hypothesis tests shown in Tables 3–5 were obtained. The results showed that alloy 0 and alloy 1 had no significantly different behavior, while alloy 2 showed a lower wear rate.

Table 3. Contrast of hypothesis for alloy 0 and alloy 1.

-	Alloy 0	-	Alloy 1
Mean	206.99	-	216.58
Variance	1094.03	-	1101.74
N	20	-	20
EE(x)	7.4	-	7.42
EE(x ₁ -x ₂)	-	10.48	-
Degree of freedom	-	38	-
t(0.975, gl)	-	2.34	-
Confidence interval	-	-9.59	±24.48

Table 4. Contrast of hypothesis for alloy 0 and alloy 2.

-	Alloy 0	-	Alloy 2
Mean	206.99	-	178.33
Variance	1094.03	-	1448.73
N	20	-	20
EE(x)	7.4	-	8.51
EE(x ₁ -x ₂)	-	11.28	-
Degree of freedom	-	37.27	-
t(0.975, gl)	-	2.34	-
Confidence interval	-	28.66	±26.34

Table 5. Contrast of hypothesis for alloy 1 and alloy 2.

-	Alloy 1	-	Alloy 2
Mean	216.58	-	178.33
Variance	1101.74	-	1448.73
N	20	-	20
EE(x)	7.42	-	8.51
EE(x ₁ -x ₂)	-	11.29	-
Degree of freedom	-	37.31	-
t(0.975, gl)	-	2.34	-
Confidence interval	-	38.22	±26.38

4. Conclusions

Ten manganese steel castings with different contents of carbon, manganese, copper, molybdenum, and chromium were obtained in order to determine if any would perform better than the material that is usually used in the manufacturing of mill wedges.

They were tested at temperatures between 100 and 900 °C, and the evolution of their microstructure and hardness was studied. With these preliminary laboratory analyses, the aim was to reduce the initial proposal to the two most appropriate alloys to carry out real tests in the mills.

Alloys 1 and 2 were chosen because they showed a smaller increase in hardness at high temperatures and greater structural stability.

These two alloys and a commercial alloy were tested in-service over 25 months in order to evaluate mass loss and wear rate. A statistical study of wear rate data using a hypothesis test showed that alloy 2 had a great resistance to wear than the other two.

Alloys 0 and 1 displayed similar behaviors, which suggests that alloy 1 does not provide any improvement.

In summary, these results reveal that alloy 2 is a good alternative to commercial alloys used in coal mill coatings.

Author Contributions: B.D.R.L. was performed data curation and formal analysis, B.D.R.L., A.I.G.D. and J.L.M.B. was made the main investigation, the methodology was conducted for all the authors, the tasks were supervising by B.D.R.L. and A.I.G.D., the visualization and validation by A.I.G.D. and J.L.M.B., and the writing, review and editing of the document by J.L.M.B., C.C.F. and A.F.V.

Funding: This research received no external funding.

Conflicts of Interest: The authors declare no conflicts of interest.

References

1. El-Bitar, T.A.; El-Banna, E.M. Improvement of austenitic hadfield Mn-steel properties by thermomechanical processing. *Can. Metall. Q.* **2000**, *39*, 361–368. [[CrossRef](#)]
2. Astudillo, P.C.; Soriano, A.F.; Barona, M.; Sánchez, H.; Ramos, J.; Durán, J.F.; Pérez, G.A. Comparative Study of the Mechanical and Tribological Properties of a Hadfield and a Fermanal steel. In Proceedings of the 15th Latin American Conference on the Applications of the Mössbauer Effect (LACAME 2016), Panama City, Panama, 13–18 November 2016.
3. Kaya, E.; Ulutan, M. Tribological and mechanical properties of deep cryogenically treated medium carbon micro alloy steel. *Met. Mater. Int.* **2017**, *23*, 691–698. [[CrossRef](#)]
4. Lee, W.S.; Wang, B.K. A study of the impact deformation and fracture behavior of austenitic manganese steel. *Met. Mater. Int.* **2006**, *12*, 459. [[CrossRef](#)]
5. Shih, C.H.; Averbach, B.L.; Cohen, M. *Work Hardening and Martensite Formation in Austenitic Manganese Alloys*; Wright Air Development Center, Massachusetts Institute of Technology: Cambridge, MA, USA, 1955.
6. Zhang, F.C.; Lei, T.Q. A study of friction-induced martensitic transformation for austenitic manganese steel. *Wear* **1997**, *212*, 195–198. [[CrossRef](#)]

7. Xu, X.L.; Yu, Z.W.; Ma, Y.Q.; Wang, X.; Shi, Y.Q. Martensitic transformation and work hardening of metastable austenite induced by abrasion in austenitic Fe-C-Cr-Mn-B Alloy—a TEM study. *Mater. Sci. Technol.* **2002**, *18*, 1561–1564. [[CrossRef](#)]
8. Fernández, J.E.; Vijande, R.; Tucho, R.; Rodríguez, J. Effect of cold deformation on the abrasive resistance of coatings with applications in the mining industry. *Wear* **2001**, *250*, 28–31. [[CrossRef](#)]
9. Kopac, J. Hardening phenomena of Mn-austenite steels in the cutting process. *J. Mater. Process. Technol.* **2001**, *109*, 96–104. [[CrossRef](#)]
10. Machado, P.C.; Pereira, J.I.; Penagos, J.J.; Yonamine, T.; Sinatora, A. The effect of in-service work hardening and crystallographic orientation on the micro-scratch wear of Hadfield steel. *Wear* **2017**, *376*, 1064–1073. [[CrossRef](#)]
11. Agunsoye, J.O.; Talabi, S.I.; Bello, O. Wear characteristics of heat-treated Hadfield austenitic manganese steel for engineering application. *Adv. Prod. Eng. Manag.* **2015**, *10*, 97. [[CrossRef](#)]
12. Zhongliang, S.; Mingyuan, G.; Junyou, L.; Yausheng, Y. High manganese steel alloying process and its influence on microstructure and properties of the steel. *J. Mater. Sci. Technol. (China)(USA)* **1995**, *11*, 102–108.
13. Lee, W.S.; Chen, T.H. Plastic deformation and fracture characteristics of Hadfield steel subjected to high-velocity impact loading. *Proc. Inst. Mech. Eng. Part C J. Mech. Eng. Sci.* **2002**, *216*, 971–982. [[CrossRef](#)]
14. Wang, K.; Du, X.D.; Youn, K.T.; Hayashi, Y.; Gyu, C.; Bon, L.; Koo, H. Effect of impact energy on the impact-wear properties of low carbon high manganese alloy steels in corrosive conditions. *Met. Mater. Int.* **2008**, *14*, 689. [[CrossRef](#)]
15. Jiang, Z.Q.; Fu, H.G.; Yin, E.S.; Tian, Y.T. Investigation and application of high strength low alloy wear resistant cast steel. *Mater. Technol.* **2011**, *26*, 58–61. [[CrossRef](#)]
16. Takacs, L.; McHenry, J.S. Temperature of the milling balls in shaker and planetary mills. *J. Mater. Sci.* **2006**, *41*, 5246–5249. [[CrossRef](#)]
17. Schmidt, R.; Scholz, H.M.; Stoll, A. Temperature progression in a mixer ball mill. *Int. J. Ind. Chem.* **2016**, *7*, 181–186. [[CrossRef](#)]
18. McKissic, K.S.; Caruso, J.T.; Blair, R.G.; Mack, J. Comparison of shaking versus baking: Further understanding the energetics of a mechanochemical reaction. *Green Chem.* **2014**, *16*, 1628–1632. [[CrossRef](#)]
19. Larson, F.R.; Miller, J. A time-temperature relationship for rupture and creep stresses. *Trans. ASME* **1952**, *74*, 765–775.
20. El-Mahallawi, I.; Abdel-Karim, R.; Naguib, A. Evaluation of effect of chromium on wear performance of high manganese steel. *Mater. Sci. Technol.* **2001**, *17*, 1385–1390. [[CrossRef](#)]
21. García, A.; Río, C.; Varela, A.; Naya, S.; Losada, R.; García, L. Influencia del cromo y el carbono en el comportamiento tribológico de aleaciones férricas. *Rev. Metal.* **2005**, *41*, 493–497. [[CrossRef](#)]
22. Higuera, O.F.; Tristancho, J.L.; Flórez, L.C. Fundamentosteoricos de los acerosausteniticos al manganeso (aceroshadfield). *Sci. Tech.* **2007**, *1*, 231–236.
23. García, A.; Varela, A.; Mier, J.L.; Camba, C.; Barbadillo, F. Estudiotribológico de acerosausteniticos tipo Hadfield: influencia del manganeso en su respuesta frente al desgaste. *Rev. Metal.* **2010**, *46*, 47–52. [[CrossRef](#)]
24. Olawale, J.O.; Ibitoye, S.A.; Shittu, M.D. Workhardening behaviour and microstructural analysis of failed austenitic manganese steel crusher jaws. *Mater. Res.* **2013**, *16*, 1274–1281. [[CrossRef](#)]
25. Hosseini, S.; Limooei, M.B. Optimization of heat treatment to obtain desired mechanical properties of high carbon Hadfield steels. *World Appl. Sci. J.* **2011**, *15*, 1421–1424.
26. García, A.; Varela, A.; García, L.; Río, M.C.; Naya, S.; Suárez, M. Comparing the tribological behaviour of an austenitic steel subjected to diverse thermal treatments. *Wear* **2005**, *258*, 203–207. [[CrossRef](#)]
27. Prishchepa, M.P.; Karpo, V.I.; Kolesniko, A.F. Effect of tempering on the properties of cast Hadfield steel G13L. *Met. Sci. Heat Treat.* **1962**, *2*, 237–238. [[CrossRef](#)]
28. Khan, A.F.; Rana, A.; Islam, M.; Abbas, T. Microstructural changes in Hadfield steel. *Pak. J. Appl. Sci.* **2001**, *1*, 317–320.

29. Fadhila, R.; Jaharah, A.G.; Omar, M.Z.; Haron, C.H.C.; Ghazali, M.J.; Manaf, A.; Azhari, C.H. Austenite formation of steel-3401 subjected to rapid cooling process. *Int. J. Mech. Mater. Eng.* **2007**, *2*, 150–153.
30. Welch, B.L. The generalization of 'student's' problem when several different population variances are involved. *Biometrika* **1947**, *34*, 28–35. [[CrossRef](#)] [[PubMed](#)]



© 2018 by the authors. Licensee MDPI, Basel, Switzerland. This article is an open access article distributed under the terms and conditions of the Creative Commons Attribution (CC BY) license (<http://creativecommons.org/licenses/by/4.0/>).